Development of Fully Implantable Retinal Prosthesis with 3-Dimensionally Stacked LSI

Tetsu Tanaka

Associate Professor
Department of Bioengineering and Robotics, Graduate School of Engineering
E-mail: ttanaka@sd.mech.tohoku.ac.jp

Abstract

To restore visual sensation of blind patients, we have proposed and developed a fully implantable retinal prosthesis with 3-dimensionally stacked retinal prosthesis chip. The retinal prosthesis chip consists of several LSI chips that are vertically stacked and electrically connected by using 3-D integration technology. Our retinal prosthesis chip has small size, light weight, and high resolution, which leads to high quality of life (QOL) to the patients.

In this study, we fabricated the retinal prosthesis module which is composed of retinal prosthesis chip, flexible cable, and stimulus electrode array. Our retinal prosthesis chip showed no characteristic degradation after module fabrication process. For the first time, we successfully implanted the retinal prosthesis module into a rabbit eyeball. We also fabricated various kinds of stimulus electrodes with different sizes and materials, and verified low impedance characteristics with porous materials such as Pt-b and Ir-b. Moreover, we fabricated and evaluated both coils and schottky barrier diode for power transmission between extra- and intraocular units in the fully implantable retinal prosthesis.

1. Introduction

Recently, several million patients become blind due to diseases such as retinitis pigmentosa (RP) and age-related macular degeneration (AMD) in the world. The RP and AMD result from impairment of photoreceptor cells that convert optical signals to electrical signals in retina. However, effective medical treatments for RP and AMD have not been established yet. While the photoreceptor cells degenerate with RP and AMD, many other retinal cells (bipolar, horizontal, amacrine, and ganglion) remain normally [1]. Accordingly, it will be possible to recover one's vision with electrically stimulating the remaining retinal cells. Many studies for retinal prosthesis are in progress worldwide at the present time [2-4].

Figure 1 shows a conventional retinal prosthesis configuration. There are three key components such as photodetector, signal processing circuit, and stimulus current generator with stimulus electrode array. The photodetector receives optical signals and converts these optical signals into electrical signals. The processing circuits perform image processing such as edge extraction and motion detection by using electrical signals. The stimulus current generator placed on the surface of retina generates appropriate patterns of electrical current, and stimulus electrode array stimulates remaining retinal cells. When the remaining retinal cells are activated by the stimulus current, blind patients would perceive a dot of light at each stimulating point.

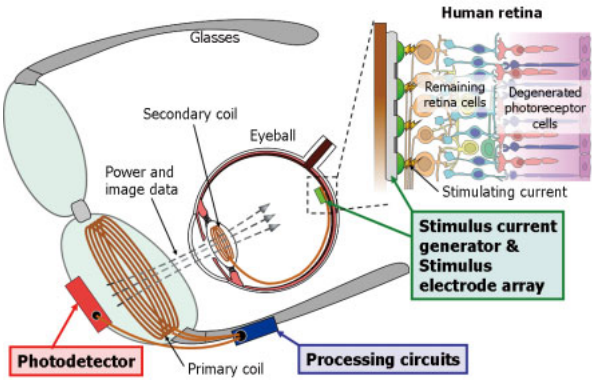

Fig. 1. Configuration of conventional retinal prosthesis

In the conventional retinal prosthesis, the stimulus current generator with tens of pixels is implanted in the eyeball, which is due to a small retinal area of ~3mm^2 suitable for retinal chip implantation. As the photodetector and signal processing circuits are placed outside the eyeball, the conventional retinal prosthesis is large, heavy, and complicated. Moreover, the patients cannot use saccadic effects based on high speed eyeball movement. These disadvantages lead a low QOL to the patients.

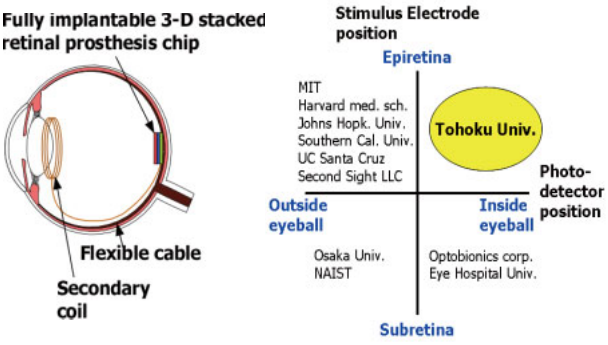

Fig. 2. Conceptual drawing of fully implantable retinal prosthesis with 3-D stacked LSI and classification of retinal prostheses

We have been developing a three-dimensional (3-D) stacked retinal prosthesis chip by using the 3-D integration technology [5,6]. Figure 2 shows a conceptual drawing of our 3-D stacked retinal prosthesis, where all key components are vertically stacked into one chip and completely implanted on the surface of retina, unlike other group's retinal prostheses. By implanting the 3-D stacked retinal prosthesis chip into the eyeball, the patients can employ their own lens and cornea, and can shift a gaze point by moving the eyeball, which leads to high speed visual information processing by using saccadic effects. The 3-D stacked retinal prosthesis chip has layered structure similar to human retina, as shown in Fig. 3. Therefore, photodetectors with more than 1000 pixels can be fabricated at the top layer of the 3-D stacked chip, leading to small size, light weight, large fill-factor, high resolution, and the resultant high QOL.

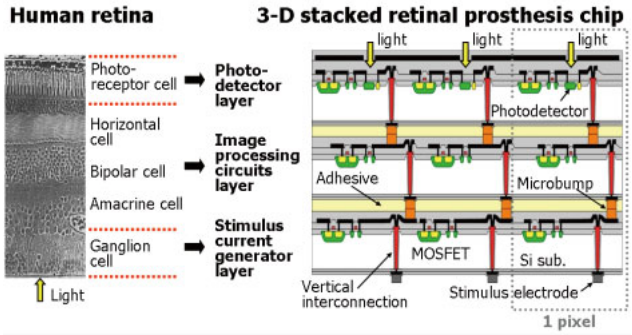

Fig. 3. Structural similarity between human retina and 3-D stacked retinal prosthesis chip

In this paper, we studied the retinal prosthesis module composed of a retinal prosthesis chip and the flexible cable with stimulus electrode array. We also investigated electrical characteristics of various kinds of stimulus electrode, and power transmission characteristics with coils and schottky barrier diode.

2. Design of Retinal Prosthesis Chip

Figure 4 shows biphasic current pulses which are usually used to stimulate retinal cells. Cathodic current pulses activate retinal cells while anodic current pulses keep charge balance. It is very important for the patients to optimize parameters of stimulus current individually. Therefore, we designed pixel circuits so that we can adjust current pulse waveforms with BIAS voltages, as shown in Fig. 5. This pixel circuit consists of photodetector, anodic pulse controller, cathodic pulse controller, and current pulse generator. Both cathodic and anodic current pulse durations can be controlled by adjusting BIAS2 and BIAS5 voltages, respectively. The interphase delay can be also controlled by BIAS4 voltage. For this pixel circuit, phototransistors were used for light detection.

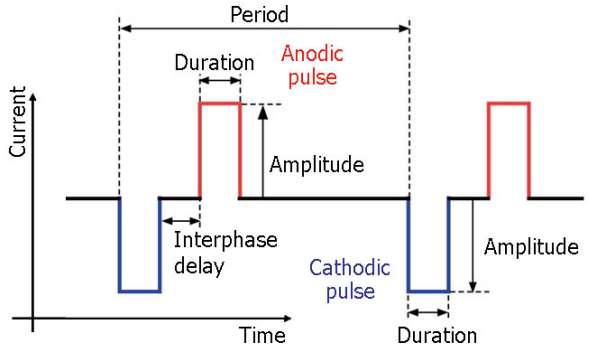

Fig. 4. Bipahsic current pulse waveform for retinal stimulation

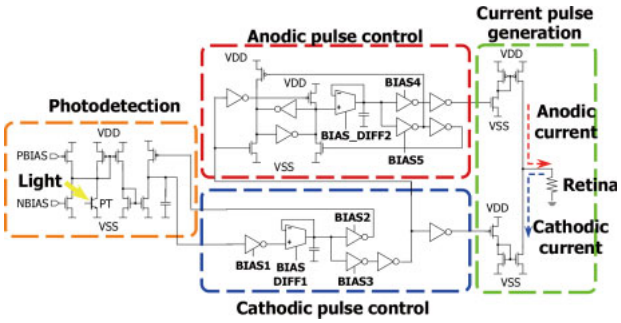

Fig. 5. Pixel circuit diagram of retinal prosthesis chip

In this study, we fabricated and used the 2-D retinal prosthesis chip as a prototype for 3-D retinal prosthesis chip. There is no functional difference between 2-D and 3-D designs, except for the area size of a pixel circuit. Figure 6 shows a photograph of the prototype 2-D retinal prosthesis chip with 16 pixels and pixel circuit layout. We used a 0.35μm double poly-Si and triple metal CMOS process technology for this retinal prosthesis chip. Each pixel has the photodetector circuit, biphasic pulse control circuit, and stimulus current generator circuit. The photo-detecting area is $20\times20\mu m^2$ in the photodetector.

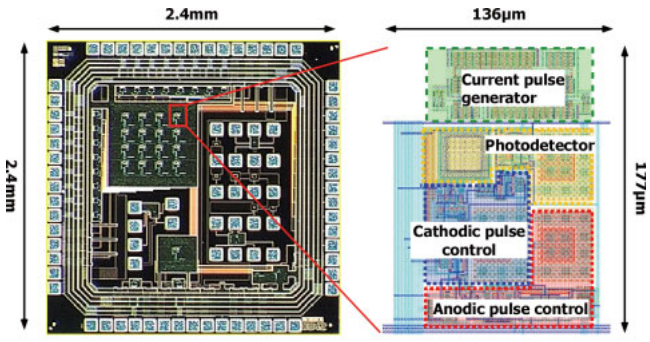

Fig. 6. Photograph of retinal prosthesis chip and pixel circuit layout

3. Fabrication and Evaluation of Retinal Prosthesis Module

In order to implant the retinal prosthesis chip into the eyeball, the chip needs to be attached on the flexible cable with stimulus electrode array. Figure 7 illustrates both the flexible cable and stimulus electrode array used for chip implantation experiments. An array of 4×4 Pt stimulus electrodes was formed at the end of flexible cable. The stimulus electrodes were placed at a pitch of 200μm. Three rings were formed and used for module fixation on the retina. One ring was inserted by a retinal tack inside the eyeball and the other two rings were sewn on the sclera outside the eyeball. At the other end of flexible cable, connection pads to a power supply were formed. Figure 8 shows fabrication process of retinal prosthesis module that is composed of stimulus electrode array, flexible cable, and retinal prosthesis chip.

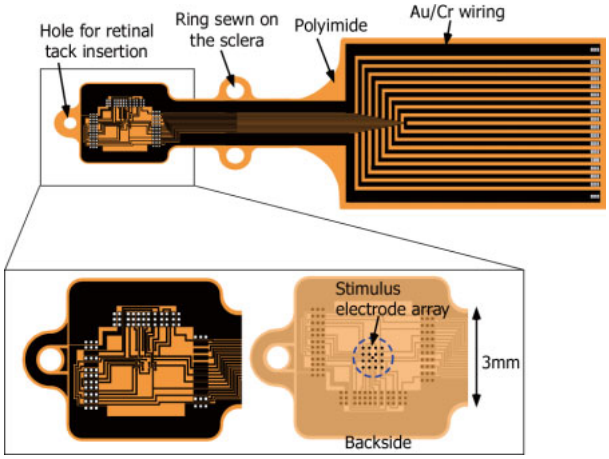

Fig. 7. Structures of flexible cable and stimulus electrode array

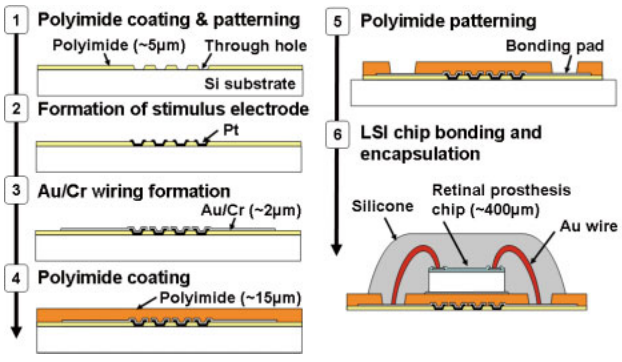

Fig. 8. Fabrication process of retinal prosthesis module

Biocompatible and photo-sensitive polyimide was employed as the flexible substrate of the cable. Pt and Au/Cr were employed for stimulus electrodes and wiring materials connected to power supply, respectively. After patterning of Au/Cr wiring, a thick polyimide was spin-coated with the thickness of 15μm. Then, bonding pads were formed by oxygen ashing. The retinal prosthesis chip was bonded on the cable with epoxy resin, and electrically connected with Au/Cr wiring by using conventional wire bonding technique. The bonded chip was encapsulated by silicone for protection from corrosive biological fluid. The photographs of the fabricated retinal prosthesis module were shown in Fig. 9. There is no silicone cap in the second photograph to see the retinal prosthesis chip clearly.

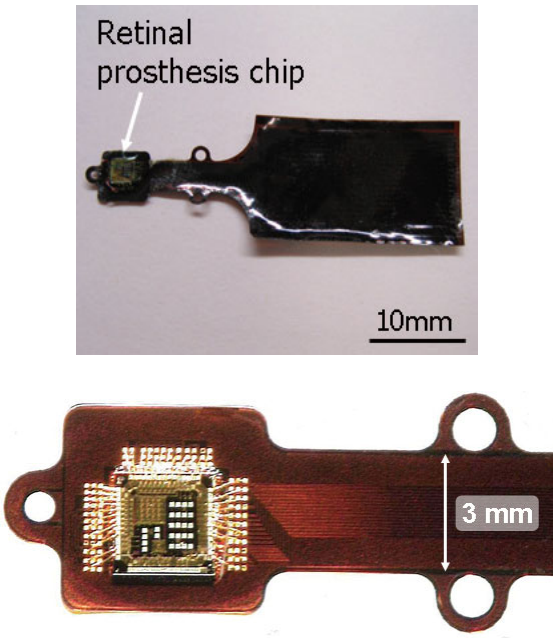

Fig. 9. Photographs of retinal prosthesis module

In order to confirm chip functions after module fabrication process, electrical characteristics were evaluated. Figures 10 and 11 show that the anodic pulse duration and the interphase delay of stimulus current pulses can be sufficiently adjusted by using BIAS voltages, respectively.

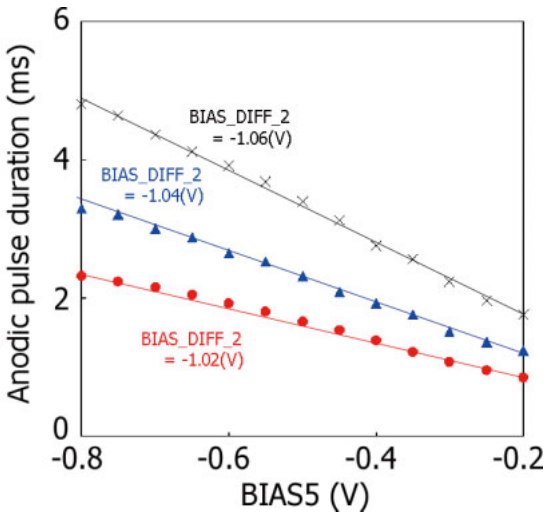

Fig. 10. Adjustment results of anodic pulse duration [Plots: measurement, Lines: SPICE simulation]

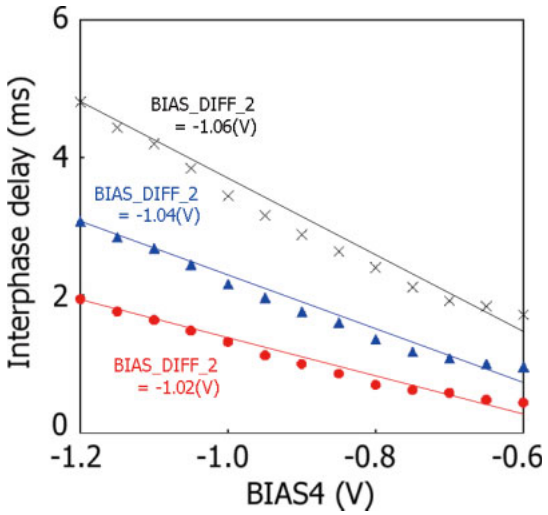

Fig. 11. Adjustment results of interphase delay [Plots: measurement, Lines: SPICE simulation]

Moreover, the incident light was successfully converted into the electrical pulse trains, and current pulse frequency can be changed in proportion to the intensity of incident light, as shown in Fig. 12. The blue symbols were measured before module fabrication process. The red symbols were measured after module fabrication process. There is no characteristic degradation by module fabrication process.

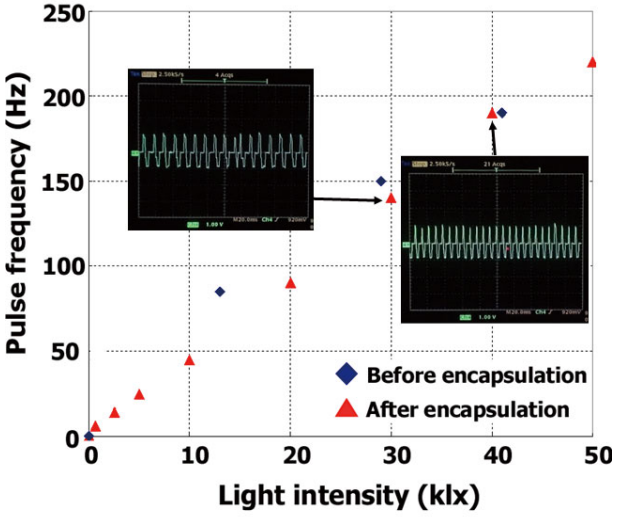

Fig. 12. Relationships between incident light intensity and generated current pulse frequency

To verify usability of the retinal prosthesis module and to optimize parameters of stimulus current pulse, it is very significant to perform fundamental animal experiments. All procedures on animal experiments in this study adhered to the Association for Research in Vision and Ophthalmology (ARVO) Resolution on the Use of Animals in Research and the guidelines of the University of California at San Francisco Committee on Animal Research. Japanese white rabbits (2-3Kg) were anesthetized with ketamine hydrochloride (66mg/kg) and xylazine hydrochloride (33mg/kg) and maintained at a surgical anesthetic level by additional injections of the mixture. In this study, the retinal prosthesis chip was completely implanted into the rabbit eyeball and fixed on the surface of retina. It is obvious that our module has sufficient endurance for implantation into the eyeball. Figure 13 shows a electrically evoked potential (EEP) recording apparatus. The EEP is the electrical potential elicited from the brain cortex when the retina is stimulated by electrical current. Pt electrodes with 4 x 4 matrixes was implanted into the rabbit eyeball and used to stimulate the rabbit retina. The EEP was recorded with three kinds of electrodes such as ground, reference, and measurement.

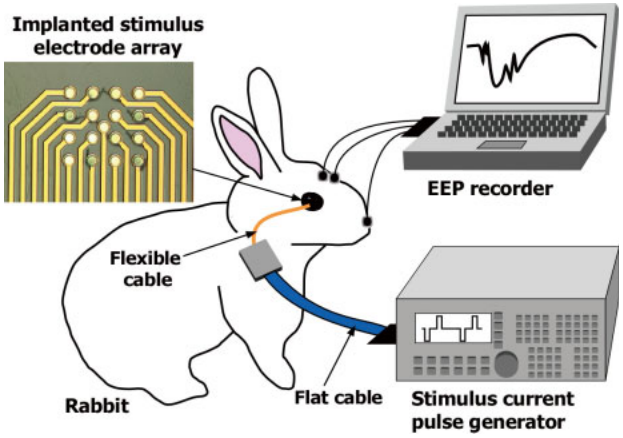

Fig. 13. Recording apparatus for electrically evoked potential (EEP) of rabbit

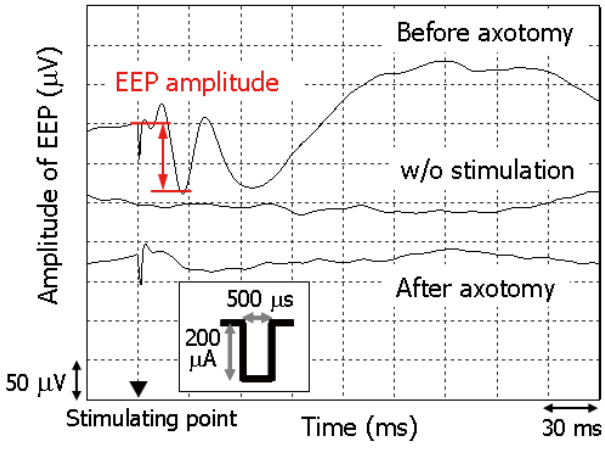

Fig. 14. EEP waveform comparison between before and after axotomy

Figure 14 compares waveforms of recorded EEP for different situation. The inset in Fig. 14 is the stimulus current pulse waveform used for the EEP recording experiments. Stimulus current pulses to elicit the EEP of the rabbit brain were applied by using implanted stimulus electrode array. There is no EEP response without electrical stimulation and with electrical

stimulation after axotomy. Therefore, the EEP response with electrical stimulation before axotomy indicates that some visual information was transferred to the primary visual cortex through the visual pathway. As results, the rabbit would perceive the light by the electrical stimulation of retina.

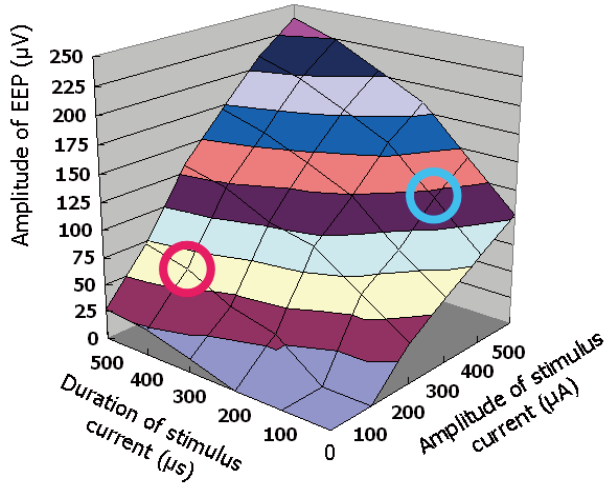

Fig. 15. Effects of both duration and amplitude of stimulus current pulse on the recorded EEP amplitude

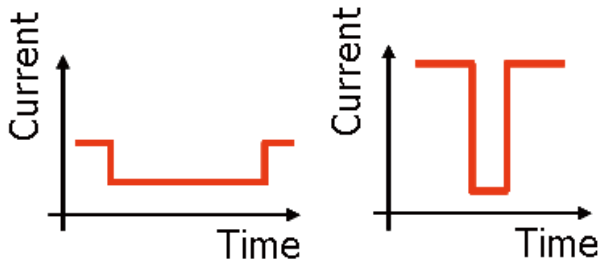

Fig. 16. Schematic drawings of stimulus current waveforms for animal experiments

Figure 15 investigates effects of both duration and amplitude of stimulus current pulse on the recorded EEP amplitude. Figure 16 shows stimulus current waveforms schematically. The left and right waveforms are identical for the conditions denoted with red circle and blue circle in Fig. 15, respectively. The amplitude of stimulus current pulse was more effective than the duration in spite of the same electrical charge quantity of stimulus current. This indicates that there would be threshold current in order to elicit the EEP signal from the brain.

4. Characteristic Study of Stimulus Electrodes

It is very important to investigate effects of both size and material on electrical property for stimulus electrodes. We fabricated various types of stimulus electrodes and measured their impedance behaviors. The diameters of stimulus electrode were within ranges from 5μm to 500μm, and the materials were Al, Au, Pt-b, and Ir-b. Fabrication procedures are shown in Fig. 17. Stimulus electrodes were formed on Si substrate with a size of 2-inch and thickness of 280μm. Si substrate was cleaned with dilute HF ($HF:H_2O = 1:200$) in order to remove natural oxides on the Si surface. Biocompatible and photo-sensitive polyimide was spin-coated on Si substrate and baked. The polyimide thickness was 25μm. 2-μm-thick Au was formed on the polyimide as metal wiring. After patterning the metal wiring with the width of 50μm, electrode material such as Al/Cr, Pt-b/Cr, and Ir-b/Cr was formed on the Au wiring by using conventional lift-off technique. Cr was used for adhesive between Au wiring and electrode material. After that, photo-sensitive polyimide with the thickness of 5μm was also spin-coated. Finally, contact holes for both electrode material and pads were formed. For the Au electrode, the lift-off process was skipped.

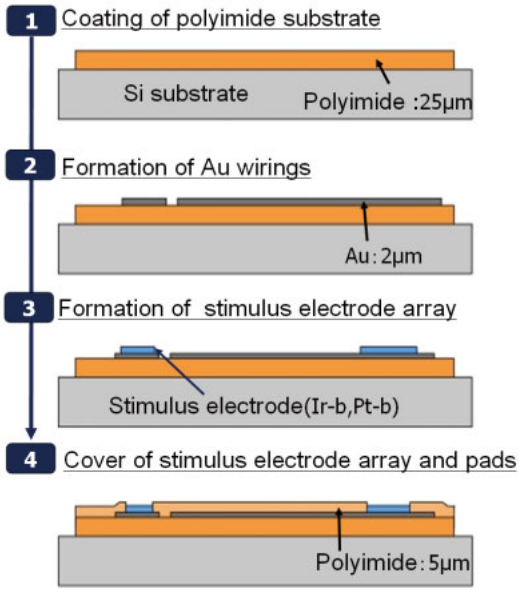

Fig. 17. Fabrication process of stimulus electrodes

Fabricated stimulus electrodes are shown in Fig. 18. There are 20 stimulus electrodes with different diameters and the same material. Stimulus electrodes are connected to pads with Au wirings. In order to investigate surface condition, the stimulus electrode surface was analyzed with laser microscope, as shown in Fig. 19. As results, the surface of Pt-b and Ir-b were rough and porous, compared to the surface of Al and Au.

Electrical characteristics for stimulus electrodes were also investigated by using impedance measurements. Measurement conditions are as follows;

Frequency: 1Hz-10MHz
Solution: 0.9% physiological saline
Reference electrode: Ag/AgCl
Counter electrode: Pt
Impedance analyzer: Solartron1260
Integration number: 100

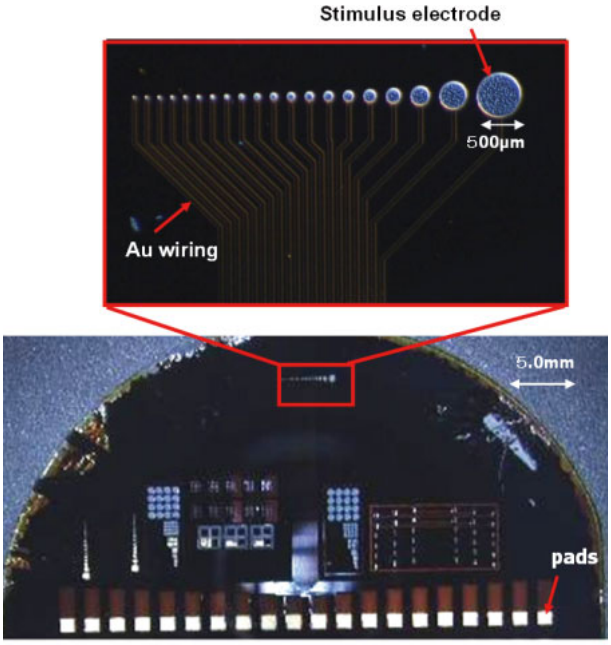

Fig. 18. Photographs of fabricated stimulus electrodes array

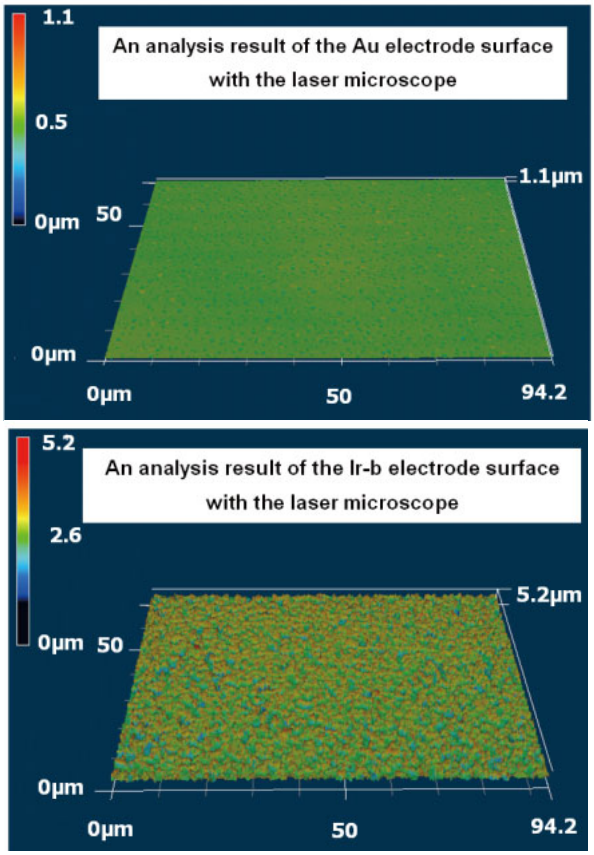

Fig. 19. Surface roughness measurement for Au (upper) an Ir-b (lower)

Relationships between frequency and impedance magnitude for different materials are shown in Fig. 20. Within frequency ranges from 100Hz to 10kHz, which is appropriate for retinal stimulation, impedance values for Pt-b and Ir-b were 2kΩ~12kΩ. From results, Al is not appropriate for retinal stimulation, due to its high impedance values. Relationships between stimulus electrode diameter and impedance magnitude for different materials at 1kHz are also shown in Fig. 21. A black dot line indicates impedance magnitude of 20kΩ. As there was electric double layer at the interface between electrode and saline, impedance magnitude decreased in accordance with the increase in both stimulus electrode area and electric double layer capacitance. Within diameter ranges from 30μm to 500μm, impedance slopes were -1.7,-1.8, and -1.9 for Ir-b, Pt-b, and Au, respectively. This phenomenon is essentially identical to surface roughness results shown in Fig. 19. To suppress irreversible reaction of stimulus electrodes, the impedance magnitude less than 20kΩ is required when the threshold current to induce action potential is 50μA. In this experiment, the diameters larger than 200μm are necessary to obtain 20kΩ, leading to small pixel number in retinal prosthesis chip. Further investigation to stimulate retinal cells is necessary.

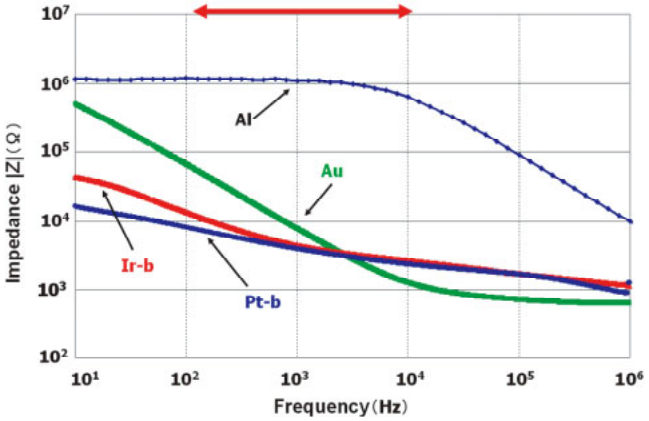

Fig. 20. Relationships between frequency and impedance for different materials

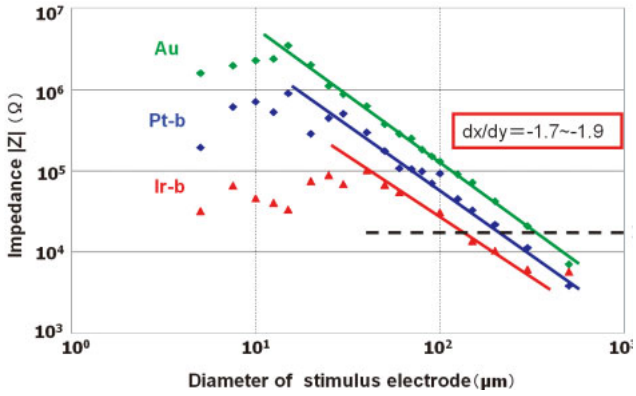

Fig. 21. Relationships between stimulus electrode diameter and impedance for different materials
(A black dot line is 20kΩ.)

5. Power Supply Units of Fully Implantable Retinal Prosthesis

5.1. Fabrication and evaluation of coil

Electromagnetic induction was employed as a power supply method to prevent eyeball from being infectious. Our power supply units are composed of a primary coil, an extraocular power supply circuit, a secondary coil placed at the eyeball, and an RF/DC voltage conversion chip for converting AC voltage to DC voltage, as shown in Fig. 22.

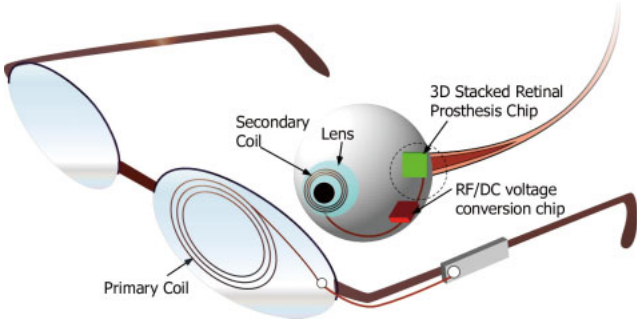

Fig. 22. Conceptual drawing for power supply units for fully implantable retinal prosthesis chip

The RF/DC voltage conversion chip has three functions, such as rectification, smoothing, and stabilization. Both the rectification and smoothing function perform the conversion of the induced AC voltages of the secondary coil into the DC voltage with ripple voltages, and the stabilization function performs the conversion of the DC voltage into the appropriate DC voltages required for the retinal prosthesis chip operation.

There are few papers reporting the power supply system suitable for the fully implantable retinal prosthesis because the human eyeball is very small and there are lots of restrictions. Regarding the power supply system for the fully implantable retinal prosthesis, this section describes the design and fabrication of the secondary coil for the power transmission and the schottky barrier diode in the RF/DC voltage conversion chip.

The present retinal prosthesis chip operates with a DC supply voltage of 3.3V. In order to receive sufficient RF peak voltages for the retinal prosthesis chip, the secondary coil has to receive the RF peak voltages of 1V higher than the DC supply voltage. Therefore, it is necessary to optimize several parameters such as an external supply voltage and transmission frequency to supply the RF peak voltage of more than 4.3V to secondary coil. Moreover, in accordance with these parameters, structural optimization is also required for the primary and secondary coils.

Fig. 23 shows the equivalent circuit diagram of extraocular and intraocular units including inductance of the secondary coil and the input resistance of retinal chip.

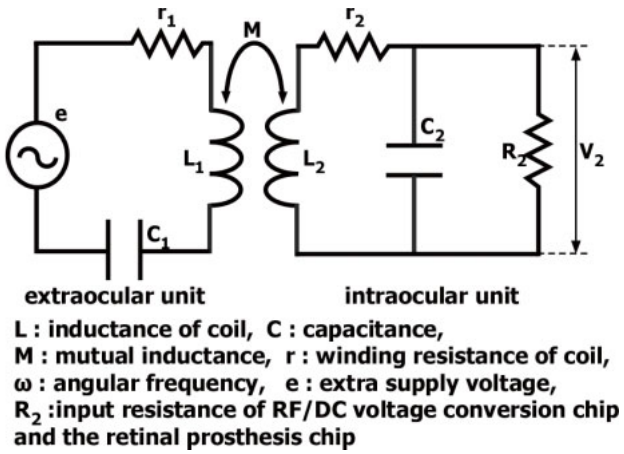

Fig. 23. The circuit diagram of extraocular and intraocular units

To improve transmission efficiency, capacitors, C_1 and C_2, are designed to resonate with coils, L_1 and L_2, respectively. The RF peak voltage V_2 can be calculated using the following formula.

$$|V_2| = \frac{\varpi M |e| R_2}{\sqrt{(r_2 r_1 + \varpi^2 M^2)^2 + (\varpi L_2 r_1 + \varpi^3 C_2 M^2 R_2 + \varpi C_2 r_2 R_2 r_1)^2}}$$

L: inductance of coil
C: capacitance
M: mutual inductance
r: winding resistance of coil
ω: angular frequency
e: external supply voltage
R_2: input resistance of the RF/DC voltage-conversion chip and the retinal prostheses chip

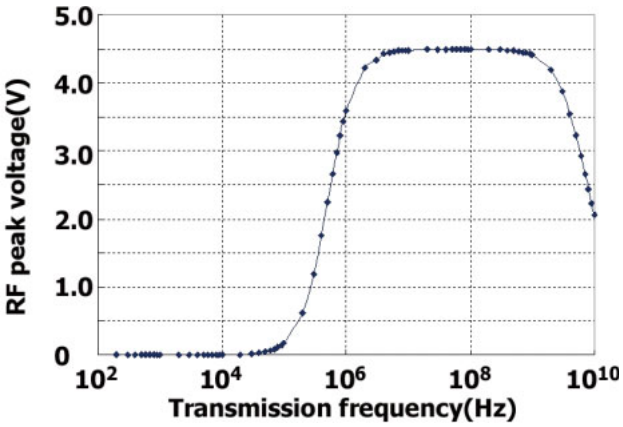

Fig. 24. Relationship between transmission frequency and RF peak voltage of a secondary coil (calculation)

A large number of turns for coils increases the mutual inductance and the resultant transmitted voltages. However, the number of turns of secondary coil is limited to 20 turns, because the secondary coil needs to be thinner so that it can be implanted in crystalline lens. Figure 24 shows the calculation results using the above equation. The RF peak voltage of 4.5 V can be obtained when we employed the primary coil with 50 turns, the secondary coil with 20 turns, the external supply voltage of 4.1 V, and the frequency ranging from 3 MHz to 300 MHz. Our power supply units using electromagnetic induction can supply the sufficient RF peak voltages for the retinal prosthesis chip.

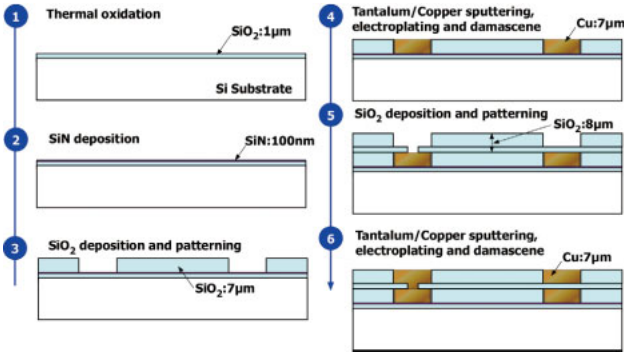

Fig. 25. Fabrication process of the secondary coil

In this study, we fabricated the secondary coil with 1 and 2 turns. The secondary coil was fabricated on a 2-inch Si substrate by using copper electroplating and damascene techniques, as shown in Fig. 25. First, silicon dioxide (SiO_2) with the thickness of 1μm was formed by thermal oxidation. Second, silicon nitride (SiN) with the thickness of 100nm was deposited as etching stop layer by the low-pressure chemical vapor deposition (LPCVD) process. After that, SiO_2 with the thickness of 7μm was deposited by the chemical vapor deposition (CVD) process and formed into the sharp of a secondary coil by buffered HF solution. Next, tantalum with the thickness of 100nm for barrier layer and copper with the thickness of 100nm for seed layer were formed by using conventional sputtering process. Then, copper was electroplated and polished. After that, SiO_2 with the thickness of 8μm was deposited by the CVD process and SiO_2 with the thickness of 7μm was removed to form into the sharp of a secondary coil by buffered HF solution. Contact holes were formed by buffered HF solution to connect copper layers. After sputtering of tantalum barrier layer and copper seed layer, second copper was electroplated and polished.

Figure 26 shows photograph and SEM cross-section of the secondary coil with 2 turns. The outer diameter and inner diameter are 10mm and 8mm, respectively. In a SEM cross-section, first copper layer and second copper layer are successfully isolated. In this case, first copper layer is thinner than target value.

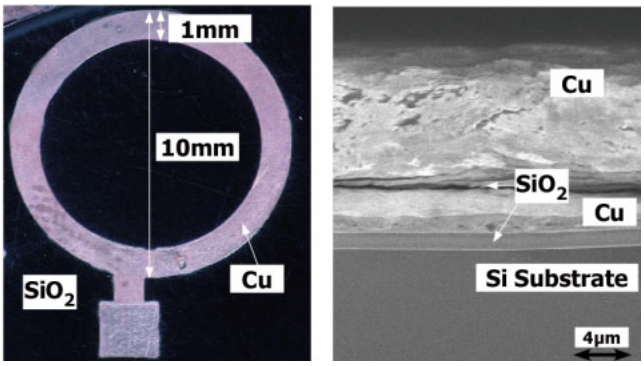

Fig. 26. Photograph and SEM cross-section of the secondary coil fabricated by using copper electroplating and damascene techniques

In order to verify inductance values of the fabricated secondary coil with 1 and 2 turns, we measured inductance values by using impedance analyzer. As shown in Fig. 27, we confirmed that secondary coils with 1 and 2 turns have the inductance values of 7nH and 19nH at 3MHz, respectively. Calculated inductance values of the secondary coil with 1 and 2 turns are 7nH and 30nH, respectively. The error of inductance value is approximately 33% for 2 turns. This is partly due to the parasitic capacitance between the first and second copper layers. From our calculation study, the secondary coil needs inductance values more than 1μH. Therefore, we are now trying to fabricate the secondary coil with optimized parameters including turn number.

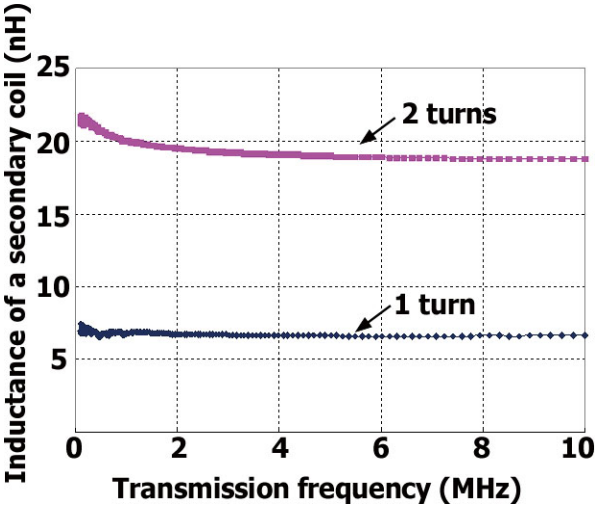

Fig. 27. Relationships between transmission frequency and inductance value for the secondary coil

5.2. Fabrication and evaluation of schottky barrier diode

In our rectifier, a bridge circuit using schottky barrier diodes was employed because the schottky barrier diode can operate with frequencies more than

3MHz. The rectifier was implemented in the RF/DC voltage conversion chip and mounted onto the flexible cable. In this study, we fabricated the schottky barrier diode bridge to rectify the RF peak voltage of secondary coil. The structure of the fabricated schottky barrier diode is shown in Figure 28. The impurity concentration of N-well at the schottky contact is an appropriate 5×10^{16} cm^{-3} and the schottky contact size is 3.3 μm by 33μm. Tungsten was employed for a metal material of schottky contact.

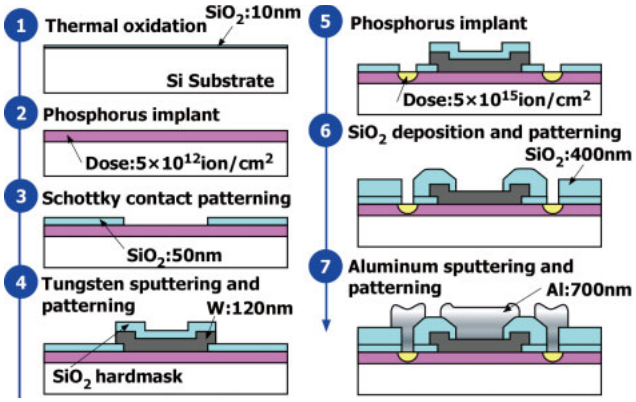

Fig. 28. Fabrication process of the schottky barrier diode

The fabrication process is shown in Fig. 28. The schottky barrier diode was fabricated on a 2-inch Si substrate by using standard photolithography techniques. First, SiO_2 with the thickness of 10nm was formed by thermal oxidation. Second, phosphorous ions were implanted with doses of 5×10^{12} cm^{-2}. After annealing at temperature of 1100 degrees Celsius, SiO_2 with the thickness of 10nm was removed by hydrofluoric treatment. Next, SiO_2 with the thickness of 50nm was formed by thermal oxidation, and the schottky contact area was also formed by conventional photolithography and etching procedures. After that, tungsten film with the thickness of 120nm was deposited by sputtering process, and SiO_2 with the thickness of 80nm was deposited as the etching mask. Following the SiO_2 patterning, tungsten film was formed by a conventional Reactive Ion Etching (RIE) process. Then, phosphorous ions were doped with doses of 5×10^{15} cm^{-2} for the N-well contact. The resistance of schottky contact was reduced by annealing after tungsten film deposition. After annealing at temperature of 900 degrees Celsius, SiO_2 with the thickness of 400nm was deposited by the CVD process. Finally, Aluminum with the thickness of 120nm was formed by sputtering and RIE processes. Figure 29 shows a photograph of the fabricated schottky barrier diode.

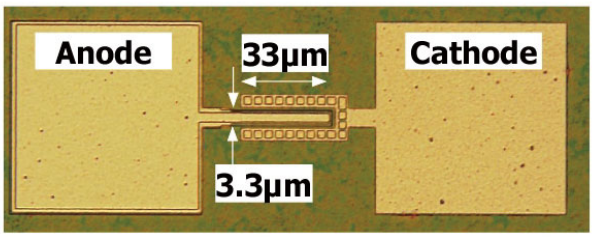

Fig. 29. Photograph of the fabricated schottky barrier diode

The breakdown voltage of the schottky barrier diode was measured for verification of electrical characteristics. As shown in Fig. 30, the breakdown voltage of fabricated schottky barrier diode was approximately 4.6V, which was sufficient for the present retinal prosthesis chip operation. In order to increase the break down voltage, the impurity concentration of N-well at the schottky contact needs to become lower.

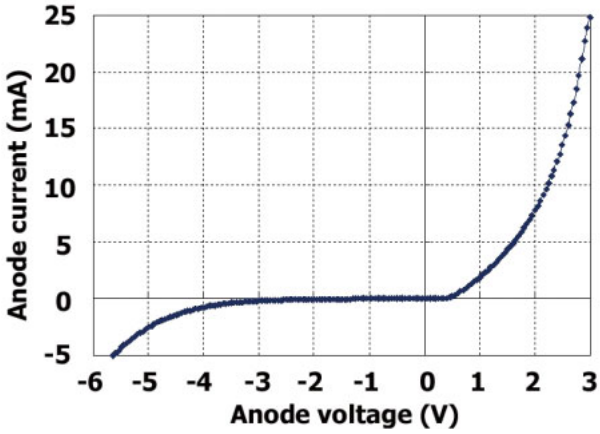

Fig. 30. The anode current-voltage characteristics of the fabricated schottky barrier diode

6. Conclusion

We successfully fabricated the fully implantable retinal prosthesis chip with photodetector and stimulus current generator bonded on the flexible cable. Our chip shows excellent electrical characteristics even after module fabrication process. For the first time, we completely implanted the retinal prosthesis chip bonded on the flexible cable with stimulus electrode array into the rabbit eyeball. In animal experiments, the recorded EEP behaviors indicate that the rabbit would perceive the light by the electrical current stimulation to retina, and that there would be threshold current to elicit the EEP from the brain.

We fabricated various types of stimulus electrodes and measured their impedance behaviors. We verified low impedance characteristics with porous materials such as Pt-b and Ir-b. In order to suppress irreversible

reaction of stimulus electrodes, it is required that electrode material has higher electrochemical limits.

The design and fabrication of the secondary coil and the schottky barrier diode in the power supply units were studied in detail. From the calculation results, we derived that the power supply units can transmit the RF peak voltage of 4.5V to a secondary coil when we employed a primary coil with 50 turns, secondary coil with 20 turns, the external supply voltage of 4.1 V, and the frequency ranging from 3MHz to 300MHz. We fabricated the secondary coil using copper electroplating and damascene techniques. We also fabricated schottky barrier diode used in the RF/DC conversion chip. The schottky barrier diode has the high breakdown voltage more than 4.5 V. Our power supply units can supply the sufficient electric power for the retinal prosthesis chip.

Acknowledgements

The author acknowledges the support of Tohoku University Global COE Program "Global Nano-Biomedical Engineering Education and Research Network Centre". This work was performed in Micro/Nano-Machining Research and Education Center, Tohoku University.

References

[1] Medeiros NE and Curcio CA. Preservation of ganglion cell layer neu-rons in age-related macular degeneration. *Investigative Ophthalmology & Visual Science* **42**, 795-803, 2001.

[2] Humayun MS, Juan E, Weiland JE, Dagnelie G, Katona S, Greenberg R, and Suzuki S. Pattern electrical stimulation of the human retina. *Vision Research* **39**, 2569-2576, 1999.

[3] Liu W, Vichienchom K, Clements M, DeMarco SC, Hughes C, McGucken E, Humayun MS, De Juan E, Weiland JD, and Greenberg R. A Neuro-Stimulus Chip with Telemetry Unit for Retinal Prosthetic Device. *IEEE Journal of Solid-State Circuits* **35**, 2569-2576, 2000.

[4] Ohta J, Yoshida N, Kagawa K, and Nunoshita M. Proposal of application of pulsed vision chip for retinal prosthesis. *Japanese Journal of Applied Physics* **41**, 2322-2325, 2002.

[5] Kurino H, Lee KW, Nakamura T, Sakuma K, Park KT, Miyakawa N, Shimazutsu H, Kim KY, Inamura K, and Koyanagi M. Intelligent image sensor chip with three dimensional structure. *International Electron Devices Meeting Technical Digest*, 879-882, 1999.

[6] Koyanagi M, Nakagawa Y, Lee KW, Nakamura T, Yamada Y, Inamura K, Park KT, and Kurino H. Neuromorphic vision chip fabricated using three-dimensional integration technology. *International Solid-State Circuit Conference Digest of Technical Papers*, 270-271, 2001.

[7] Humayun MS, Juan E, Weiland JE, Dagnelie G, Katona S, Greenberg R, and Suzuki S. Pattern electrical stimulation of the human retina. *Vision Research* **39**, 2569-2576, 1999.